The International Journal of Cardiovascular Imaging (2019) 35:1841–1851
https://doi.org/10.1007/s10554-019-01627-4

ORIGINAL PAPER

The value of the left atrial appendage orifice perimeter of 3D model based on 3D TEE data in the choice of device size of LAmbre™ occluder

Dan Jia[1] · Qing Zhou[1] · Hong-ning Song[1] · Lan Zhang[1] · Jin-ling Chen[1] · Yu Liu[2] · Bin Kong[2] · Fa-zhi He[3] · Yi-jia Wang[1] · Yuan-ting Yang[1]

Received: 30 January 2019 / Accepted: 13 May 2019 / Published online: 27 May 2019

Abstract

Preoperative optimal selection of the occluder size is crucial in percutaneous left atrial appendage (LAA) occlusion, and the maximal width of the LAA orifice is the main reference index, however it can not fully meet the practical operation requirements. We retrospectively analyzed three-dimensional (3D) transesophageal echocardiography (TEE) and computed tomography (CT) imaging dataset of the 41 patients who underwent LAA occlusion with LAmbre™ system. The LAA orifice parameters were overall evaluated to determine their role in device size selection. Eight LAA 3D models of the four cases who had been replaced their device during the procedure based on TEE and CT were printed out to verify the optimal parameter decision strategy. There was a significant concordance of the results between 3D TEE and CT in the LAA orifice evaluation. The correlations between the perimeter and maximal width measurements by 3D TEE and the closure disk of the device were stronger than that between the area measurements and the closure disk ($r = 0.93, 0.95, 0.86$, respectively and $p < 0.001$ all), and the result was similar to that by CT ($r = 0.92, 0.93, 0.84$, respectively and $p < 0.001$ all). The ratios of the maximal width to the minimal width of the four cases were all > 1.4, however the rest 37 cases were all ≤ 1.4. Based on the comprehensive assessment of the LAA orifice perimeter and maximal width of the 3D printed models, the experiments were all succeed just for one try. The LAA orifice perimeter of 3D printed model based on 3D TEE may help in choosing the optimal device size of LAmbre™, especially for the LAA with flater ostial shape.

Keywords Left atrial appendage closure · Size · Orifice · Three-dimensional transesophageal echocardiography · Computed tomography · Three-dimensional model

Abbreviations

LAA	Left atrial appendage
3D	Three-dimensional
TEE	Transesophageal echocardiography
DICOM	Digital imaging and communications in medicine
CT	Computed tomography

Introduction

Transcatheter left atrial appendage (LAA) occlusion is an effective treatment for the prevention of atrial fibrillation-related stroke in patients with anti-coagulation contraindications or a high risk of embolism [1, 2]. However, the anatomical morphology and the size of the LAA vary greatly, which makes percutaneous occlusion fairly challenging [3, 4]. In early clinical trials of LAA occlusion, interventional physicians used an average of 1.8 occluders to achieve a satisfactory sealing effect, and frequent replacement of occluders can increase the risk of complications. Improper size of LAA occluder will lead to an increased times of replacement, and oversizing and undersizing of the LAA occluder have potential risks of complications, such as device migration or embolization, cardiac perforation, pericardial effusion and even cardiac tamponade. Thus, preoperative optimal selection of the device size is particularly important to increase the one-time success rate of occlusion [5–7].

✉ Qing Zhou
qingzhou128@hotmail.com

[1] Department of Ultrasound Imaging, Renmin Hospital of Wuhan University, Wuhan, China

[2] Department of Cardiology, Renmin Hospital of Wuhan University, Wuhan, China

[3] Computer Science and Technology School, Wuhan University, Wuhan, China

Currently, the maximal width of the LAA orifice measured by clinical imaging modality is the main reference index for the clinical decision, while the anatomy of the LAA orifice can not be accurately and comprehensively assessed just by this parameter. For example, for the LAA whose opening shape is foot-like, the difference between the maximal and minimal width of the LAA orifice is large. Due to the occluders are all round-shape, as a result, the device would be more easily overestimated if only consideration of the maximal width, which may cause the difficulty of release and lead to the corresponding complications.

In recent years, studies have shown that three-dimensional (3D) printing technology has rapidly developed in the field of cardiovascular medicine [8–10]. Presently, patient-specific 3D printing LAA models based on computed tomography (CT) and 3D transesophageal echocardiography (TEE) [11–12] have been successfully applied to the guidance of percutaneous LAA occlusion, and CT is the mainstream approach. In this study, we used the Materialise interactive medical image control system (Mimics; Leuven, Belgium) to post-process the digital imaging and communications in medicine (DICOM) data from 3D TEE and cardiac CT to obtain the 3D printing digital file of the LAA, and then to compare and evaluate these measurements based on these two 3D data sources.

On this basis, our study evaluated the relationship between the several parameters of the LAA orifice of 3D models based on 3D TEE and CT data and the actually implanted device size of LAmbre™. By obtaining patient-specific 3D printed LAA models with a rubber-like material, which could simulate the deformation action after the implantation of the occluders, we intended to discuss the instruction value of LAA orifice perimeter for sizing an LAA occluder especially for those cases with special ostia shape.

Methods

Research subjects

This was a retrospective study. Forty-one patients with persistent or paroxysmal atrial fibrillation who underwent successful LAA occlusion with the LAmbre™ device in our hospital between January 2015 and February 2017 were enrolled in this study. The device sizes during LAAO in these patients were selected under the guidance of the maximal width based on 3D TEE in the 3D Flexi Slice mode at the 135° planes and X-ray. Patients with other forms of arrhythmia, coronary heart disease, cardiomyopathy, congenital heart disease, or other organic heart disease were excluded. All patients had both 3D TEE and cardiac CT images with high quality in our hospital database. Four of them had been replaced occluders once during actual occlusion, and the other 37 cases were all successfully occluded for one try. The study protocols were approved by the ethics committee at Renmin Hospital of Wuhan University.

TEE image acquisition

Patients were required to fast for 10 h prior to the examination. All of them were monitored via a synchronized electrocardiogram (ECG) and were assessed in the left lateral decubitus position. On this basis, TEE was performed on all 41 patients by experienced investigators using the GE Vivid E9 platform (GE Vingmed Ultrasound AS, Horten, Norway). The 6VT-D 3D TEE probe (3–8 MHz, frame rate: 8–12 frames/s) was placed in the middle esophagus to acquire 3D images. After obtaining a clear LAA two-dimensional gray image in the middle of the esophagus at 90°, the "4DZOOM" function was applied to tailor the LAA into the sampling box. Once the 4D mode was entered, five continuous root cycle volume images of the LAA were recorded under single-beat mode. To obtain the best image result, frame frequency and gain were set reasonably. The image was imported into the EchoPac workstation (GE Healthcare, WI).

CT image acquisition

CT images were acquired using a 64-row, 128-slice volume CT coronary angiography system (LightSpeed VCT, GE Healthcare, VA). Scanning ranged from the tracheal bifurcation level to 5 cm below the diaphragm. The scanning parameters were set as follows in the retrospective ECG gating: tube voltage 120 kV, tube current 300–650 mA, pitch 0.984, scanning layer thickness 5 mm, reconstruction layer thickness 0.625 mm. The image was stored in the GE ADW 4.6 workstation.

Image post-processing

The DICOM volume data of LAA at 75% of the R-R interphase of the cardiac cycle by 3D TEE from the EchoPac workstation was exported into MATLAB software to obtain multi-slice information. These multi-slice data-based 3D TEE and the volume data of LAA at the same cardiac cycle by CT from the GE ADW 4.6 workstations were post-processed by Mimics Innovation Suite 17.0 (Materialise, Leuven, Belgium) to obtain a 3D volume image of the LAA. The main related operations included gray-scale inversion, threshold segmentation, editing of the 3D mask (area of interest of the contour mask), manual denoising process of interactive segmentation and 3D model calculation (Fig. 1).

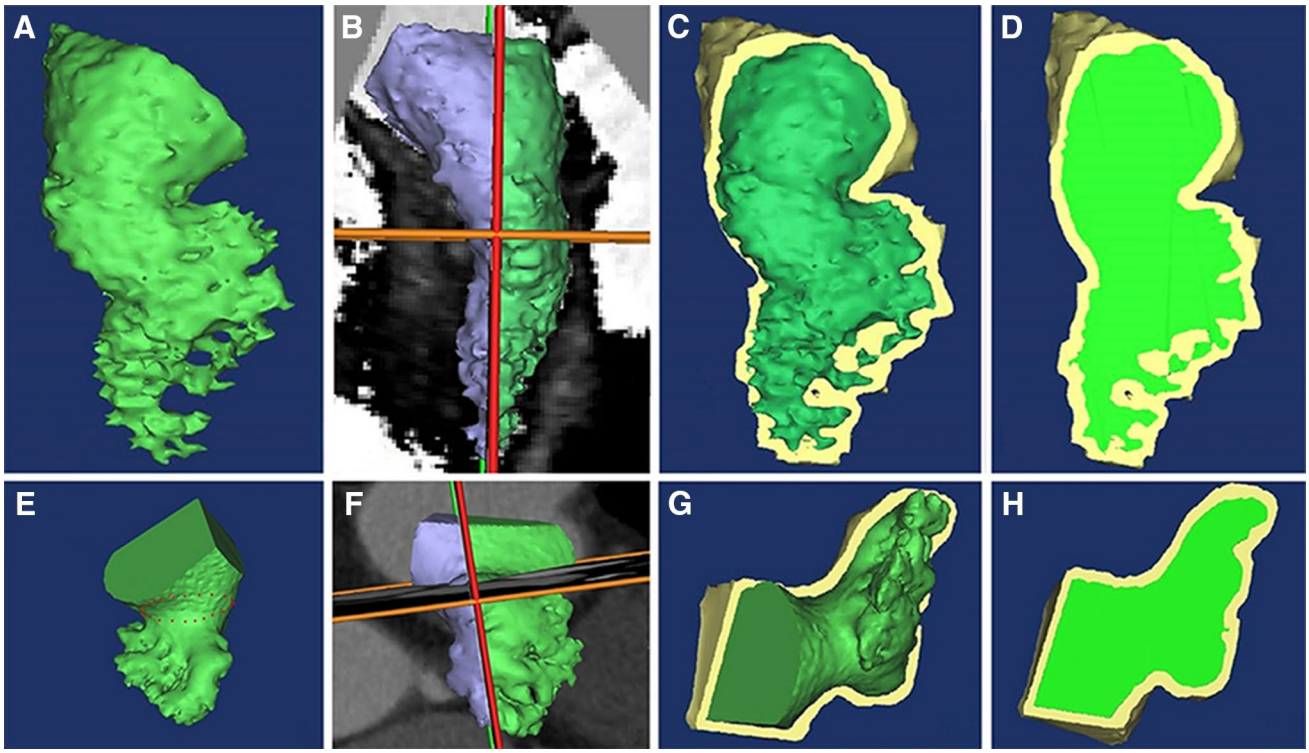

Fig. 1 The three-dimensional (3D) reconstruction images based on 3D transesophageal echocardiography (TEE) (**a**–**d**) and computed tomography (CT) (**e**–**h**). **a** and **e** show the left atrial appendage (LAA) cardiac chamber model. **b** and **f** show the 3D cutting of three orthogonal planes. **c**, **d**, **g** and **h** show the LAA cardiac wall model

Measurement and evaluation of the anatomical parameters of the LAA orifice

Qualitative parameters: according to the shape of the LAA orifice, the ostial morphology was classified into the following five imaging types: oval, foot-like, triangular, water drop-like and round. The acquisition process of the orifice is described in the next section.

Quantitative parameters: multi-planner reconstruction (MPR) was applied to the mask of the LAA, which had been calculated. By rotating three mutually perpendicular planes, the reconstructed orifice plane of the LAA was obtained 10 mm distally from the ostial plane (at the junction of the left atrium and the LAA) into the lobe. The maximal width, minimal width, perimeter, and area of the LAA orifice were measured and the shape of the LAA orifice was recorded in the corresponding MPR plane (Fig. 2).

Simulation operation

The final DICOM volume data were converted into stereolithography files. Eight life-sized LAA models based on 3D TEE and CT dataset were printed out using a rubber-like material, which were the four cases who had been replaced devices during actual implantation, the maximal width, minimal width and perimeter of the LAA orifice were measured by vernier caliper, and the shape of the LAA orifice was recorded. Simulation operations with the LAmbre™ device were performed on the models by the assessment of the size of the LAA orifice.

Observer variability

All the data were post-processed by two physicians with more than 100 cases of LAA data analysis experience in a randomized double-blind trial. The data were analyzed two days apart by the same observers who were blinded to their first results, and the average value was used for statistical analysis.

Statistical analysis

Statistical analyses were performed using SPSS version 21.0 (SPSS, Chicago, IL) and MedCalc version 11.0.1.0 (MedCalc Software, Mariakerke, Belgium). Continuous variables were presented as the means ± standard deviations, and categorical variables were presented as frequencies or percentages. Paired t tests were used to compare differences between different methods. The data on the LAA orifice based on 3D TEE and CT and the final implanted device

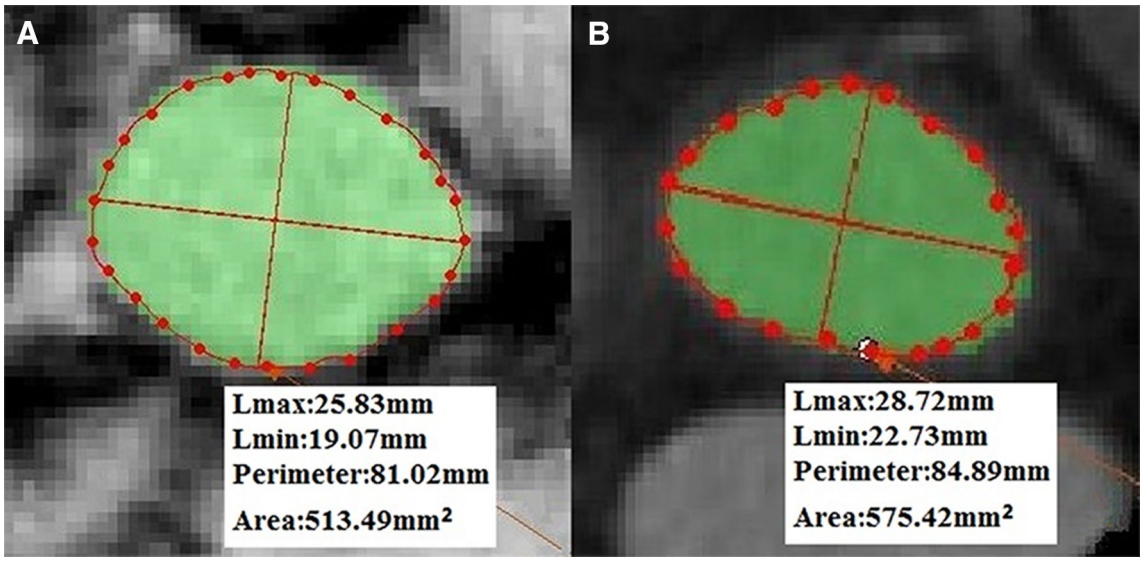

Fig. 2 The measuring method of the maximal width, minimal width, perimeter and area of the left atrial appendage (LAA) orifice based on three-dimensional (3D) transesophageal echocardiography (TEE) (**a**) and computed tomography (CT) (**b**)

size were analyzed to assess the normality of the distribution using Kolmogorov–Smirnov tests. The agreement between different measurements by the two methods was expressed by the Lin concordance coefficient. The equivalence of the measurements by these two methods was investigated using Bland–Altman agreement and graphically presented as Bland–Altman plots. A kappa test was used to assess the agreement of LAA morphological parameters by 3D TEE and CT, and the agreement was weighted according to the frequency of opening shape type. The association between measurements of the parameters of the LAA orifice in the 41 cases via the two methods and the final implanted device size was assessed by the Pearson correlation coefficient. Inter-observed and intra-observed agreement were analyzed by the intra-class correlation coefficient. *p*-Values below 0.05 were considered significant.

Results

3D DICOM LAA data by echo and CT were successfully post-processed in 41 patients (Table 1), and the anatomical parameters of the LAA orifice were measured and evaluated (Table 2; Fig. 3).

Comparison and evaluation of different ostial parameters between 3D TEE and CT

Qualitative parameters: shape of the LAA orifice: There were three types assessed via 3D TEE, as follows: oval in 34 cases (82.9%), round in two cases (4.9%) and water drop-like in five cases (12.2%). Four types were observed by CT, as follows: oval in 35 cases (85.4%), round in two cases (4.9%), water drop-like in two cases (4.9%), and triangular in two cases (4.9%) (Fig. 4). The kappa value was 0.742 with good agreement.

Quantitative parameters: CT-based measurements of the maximal width (mm), minimal width (mm), perimeter (mm), and area (mm^2) of the LAA orifice were larger than those by 3D TEE (all $p < 0.05$).

The correlation between the maximal width, minimal width, perimeter, and area of the LAA orifice via 3D TEE and CT using Lin's concordance coefficient were 0.91 (95% CI 0.85, 0.95), 0.87 (95% CI 0.78, 0.93), 0.81 (95% CI 0.70, 0.89), and 0.92 (95% CI 0.86, 0.95), respectively. Bland–Altman plots demonstrated good agreement between these four parameters by the two methods, with mean differences of 1.6 mm (95% LOA-1.2, 4.4), 1.1 mm (95% LOA-1.9, 4.1), 6.8 mm (95% LOA-5.1, 18.8), and 50.0 mm^2 (95% LOA-38.1, 138.2), respectively. The majority of plots (95.1%, 97.6%, 92.7%, and 95.1%, respectively) fell within the limits of agreement.

Correlation between the measurements of the ostial parameter of 3D LAA models and the actually inserted occluder size

Correlations between the values of the perimeter (mm), maximal width (mm), and area (mm^2) of the closure disk of the finally implanted LAmbre™ device and the 3D TEE-based results in 41 cases were $r = 0.93$, $p < 0.001$; $r = 0.95$, $p < 0.001$; $r = 0.86$, $p < 0.001$, respectively, and the result was similar to that by CT($r = 0.92$, $p < 0.001$; $r = 0.93$, $p < 0.001$; $r = 0.84$, $p < 0.001$, respectively).

Table 1 The clinical information of 41 patients with LAAO

Number	Max W	Min W	EI	Shape of the LAA orifice by 3D TEE	Occluder replacement during LAAO/numbers	Device size in the first choice	Device size in the second choice
1	20.22	15.2	1.33	Oval	No	32/26	
2	32.98	23.85	1.38	Oval	No	40/36	
3	28.21	24.31	1.16	Oval	No	38/34	
4	21.56	20.15	1.07	Oval	No	32/26	
5	24.6	18.38	1.34	Oval	No	32/26	
6	31.63	30.16	1.05	Oval	No	40/36	
7	25.83	19.07	1.35	Oval	No	34/28	
8	22.39	16.42	1.36	Water drop-like	No	32/26	
9	26.12	19.35	1.35	Oval	No	36/30	
10	24.24	17.5	1.39	Oval	No	36/30	
11	17.76	17.03	1.04	Round	No	28/22	
12	32.78	22.24	1.47	Oval	Yes/1	40/36	38/34
13	30.76	18.19	1.69	Water drop-like	Yes/1	38/34	36/32
14	15.59	12.18	1.28	Oval	No	26/20	
15	18.69	15.19	1.23	Oval	No	28/22	
16	29.74	21.37	1.39	Oval	No	38/34	
17	18.38	13.97	1.32	Oval	No	26/20	
18	15.51	15.24	1.02	Oval	No	30/16	
19	26.37	21.96	1.2	Oval	No	36/30	
20	19.59	17.59	1.11	Oval	No	32/20	
21	17.37	16.13	1.08	Oval	No	30/24	
22	22.01	15.82	1.39	Oval	No	32/26	
23	33.62	26.27	1.28	Oval	No	40/36	
24	25.73	21.12	1.22	Oval	No	34/28	
25	19.96	16.02	1.25	Oval	No	28/22	
26	31.13	23.48	1.33	Oval	No	40/36	
27	31.15	20.36	1.53	Oval	Yes/1	38/34	36/32
28	21.29	16.07	1.32	Oval	No	30/24	
29	32	24.84	1.29	Oval	No	40/36	
30	21.8	17.65	1.24	Water drop-like	No	30/24	
31	23.98	17.29	1.39	Oval	No	32/26	
32	18.12	15.66	1.16	Water drop-like	No	28/22	
33	26.67	20.17	1.32	Oval	No	36/30	
34	25.61	16.24	1.58	Water drop-like	Yes/1	34/28	32/26
35	22.56	19.17	1.18	Oval	No	34/28	
36	28.5	22.44	1.27	Oval	No	36/32	
37	20.11	18.35	1.1	Oval	No	32/26	
38	20.1	19.7	1.02	Round	No	30/24	
39	26.72	21.23	1.26	Oval	No	36/30	
40	29.3	20.88	1.4	Oval	No	38/34	
41	20.44	19.45	1.05	Oval	No	30/24	

LAAO left atrial appendage occlusion, *Max W* maximal width of LAA orifice, *Min W* minimal width of LAA orifice, *EI* ellipticity index (maximal width/minimal width), *3D TEE* three-dimensional transesophageal echocardiography

Table 2 3D TEE, CT and device measurements in 41 cases

	Maximal width (mm)	Minimal width (mm)	Perimeter (mm)	Area (mm^2)
Device	27.76 ± 5.30	27.76 ± 5.30	87.20 ± 16.63	626.56 ± 231.91
3D TEE	24.42 ± 5.21	19.21 ± 3.63	69.71 ± 14.36	413.83 ± 164.05
CT	26.04 ± 4.95	20.30 ± 3.63	76.54 ± 14.03	463.88 ± 159.57

3D TEE three-dimensional transesophageal echocardiography, *CT* computed tomography

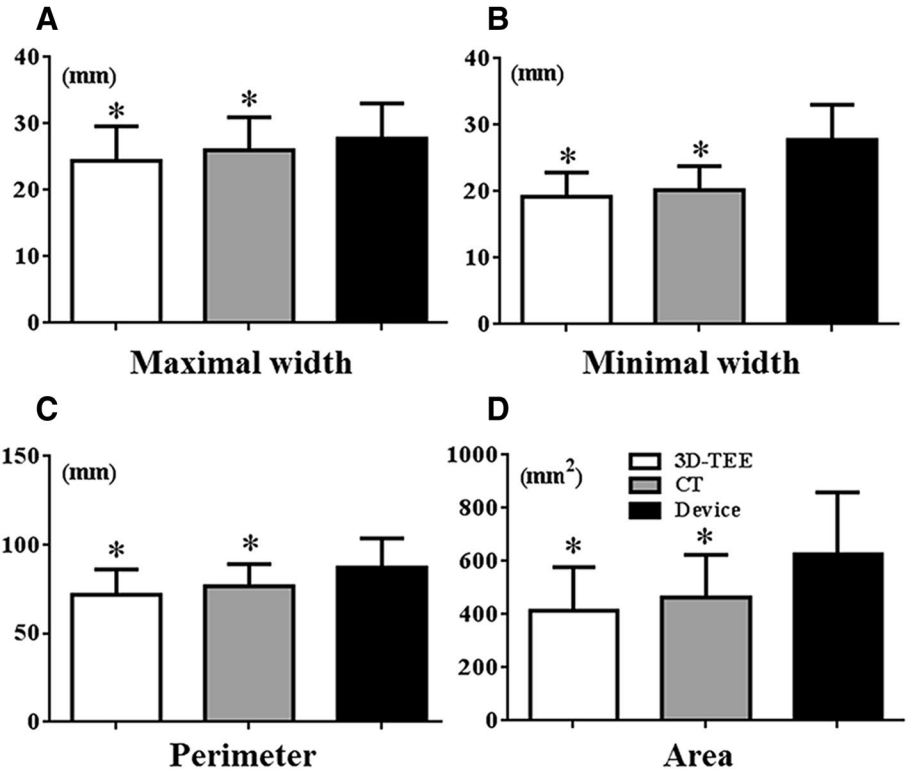

Fig. 3 Measurements of the parameters of left atrial appendage (LAA) orifice base on three-dimensional (3D) transesophageal echocardiography (TEE), computed tomography (CT) and the device size in 41 cases. *$p < 0.05$, compared with the finally implanted device size

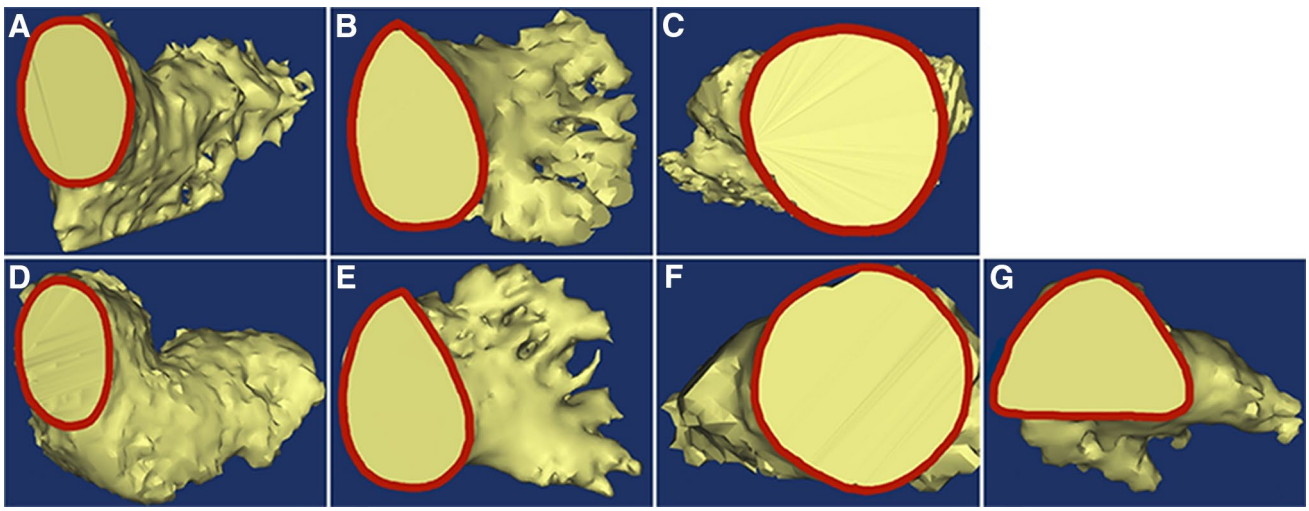

Fig. 4 Different shapes of left atrial appendage (LAA) orifice based on three-dimensional (3D) transesophageal echocardiography (TEE) and computed tomography (CT). Three types including oval (**a**), water drop-like (**b**) and round (**c**) were evaluated via 3D TEE. Four types including oval (**d**), water drop-like (**e**), round (**f**) and triangular (**g**) were assessed based on CT

Relationship between the measurements of the LAA ostial parameters and their shapes

By analysis, in the four cases who had been successfully implanted device in the second try, the ratios of the LAA ostial maximal width to the minimal width based on 3D TEE and CT were all > 1.4. However, in the other 37 cases, whose actual intervention operations were all successfully performed just for once, the values were all ≤ 1.4, and the shapes of the orifice were rounder than those in the four cases.

Simulation operation

Our research group successfully obtained eight LAA 3D printing models based on 3D TEE and CT dataset. We found that the error of the LAA ostial maximum width, minimum width and perimeter measurements of the 3D printed models (Tables 3, 4) and the corresponding results of the 3D reconstruction models was small, and the results of these two modes for sizing LAA occluders were consistent.

After a failed attempt, the simulation operation in the first model (NO.12) based on TEE data was successfully carried out in the second experiment. The maximal width of the LAA orifice was 33.01 mm. According to the principle of routine clinical selection of the device size, a 36 mm LAmbre™ occluder was selected and it was delivered within the 3D printed LAA. However, the release results showed that the size was too large, which resulted in obvious exposure of the device shoulder. The minimal width of the LAA orifice was 21.88 mm, the ratios of the LAA ostial maximal width to it was 1.51, accordingly, the difference between the minimal width and the maximal width values of the LAA orifice was high, which was in accordance with its morphologically long oval shape. Thus, in view of the above correlation results, we also analyzed the LAA ostial perimeter. The measurement of the perimeter of the LAA orifice was 80.59 mm, which was much smaller than the corresponding measurement of a 36 device (113.10 mm), but was closer to the measurement of a 34 device (106.81 mm). On this basis, the occluder was changed to a smaller size of 34 mm in the second choice, which had the same size as the occluder chosen for the actual procedure, and it demonstrated good sealing (Fig. 5). Similar situations occurred in other three LAA models based on TEE data (NO.13, 27, 34, respectively) and two models based on CT data (NO. 27 and NO. 34). In the NO.12 model based on CT, the maximal width of the LAA orifice was 33.88 mm and a 34 mm LAmbre™ was selected. The results showed good sealing. And considering that the measurement of the LAA orifice perimeter (103.32 mm) in the model was close to the corresponding measurement of the 34 mm device, the second test was not carried out. Similar situation occurred in the NO.13 LAA model.

Observer variability

Interobserver intraclass correlation coefficients for the parameters of the maximal width, minimal width, perimeter, area and shape of the LAA orifice via 3D TEE were 0.95, 0.93, 0.91, 0.93, and 0.82, respectively, and the corresponding values based on CT were 0.92, 0.90, 0.94, 0.91, and 0.85, respectively. Intraobserver intraclass correlation coefficients for the same parameters by TEE were 0.96, 0.92, 0.94, 0.95,

Table 3 The LAA ostial parameters results of the 3D printed wall models based on 3D TEE

Number	Maximal width (mm)	Minimal width (mm)	EI	Perimeter (mm)	Shape of the LAA orifice
12	33.01	21.88	1.51	80.59	Oval
13	31.25	18.77	1.66	82.81	Water drop-like
27	30.97	20.03	1.55	80.04	Oval
34	25.98	17.22	1.51	72.12	Water drop-like

EI ellipticity index (maximal width/minimal width)

Table 4 The LAA ostial parameters results of the 3D printed wall models based on CT

Number	Maximal width (mm)	Minimal width (mm)	EI	Perimeter (mm)	Shape of the LAA orifice
12	33.88	23.86	1.42	103.32	Oval
13	31.56	22.14	1.43	96.84	Water drop-like
27	32.79	21.29	1.54	81.06	Oval
34	26.94	17.27	1.56	75.11	Oval

EI ellipticity index (maximal width/minimal width)

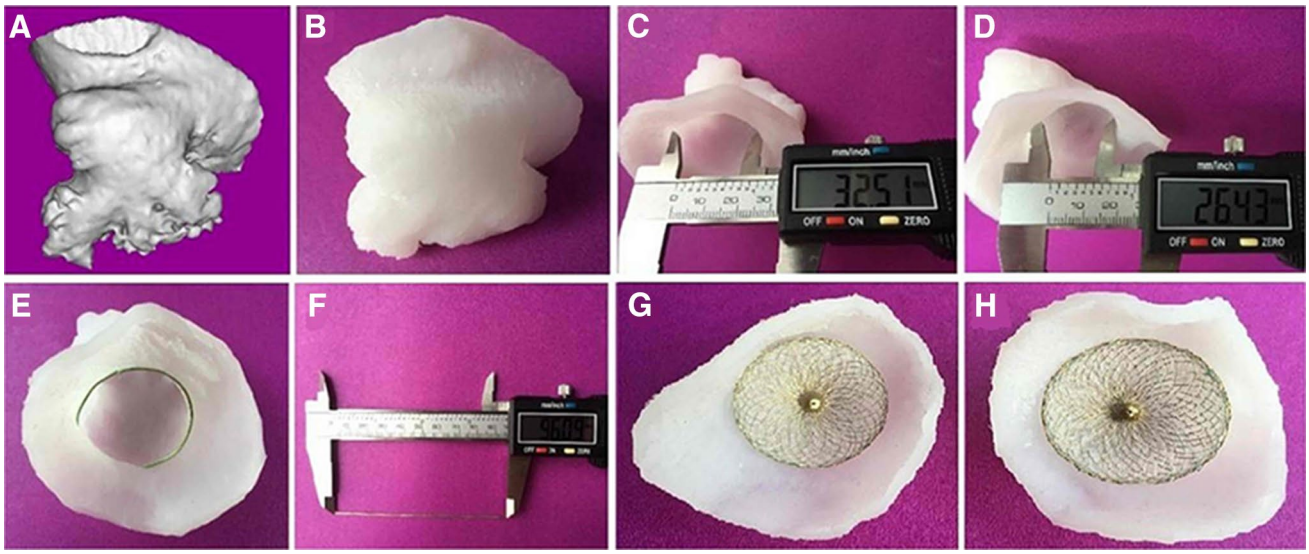

Fig. 5 The process of the simulation operations.The left atrial appendage (LAA) three-dimensional (3D) volume images were obtained through several operations such as segmentation (**a**) and the LAA 3D printed heart wall models were obtained (**b**). The maximal width (**c**), minimal width (**d**) and perimeter of the LAA orifice were measured by vernier caliper, and the measuring method of perimeter was wire moulding(**e–f**). On the basis, simulation operations were performed on the models. By comprehensive analysis of the LAA orifice parameters, especially the maximal width and perimeter, the LAmbre™ occluders finally used for simulation were selected, which had the same size as the occluders chosen for the actual procedure, and were inserted into 3D models with a near perfect fit (**g–h**)

and 0.89, respectively, and by CT were 0.97, 0.93, 0.92, 0.96, and 0.90, respectively.

Discussion

In this study, we found that 3D TEE and CT were in good concordance in assessing the LAA orifice. On this basis, we innovatively analyzed the relationship between the measurements of each LAA ostial parameter based on these two techniques and the final occluder size, and the major findings were summarized as follows: (1) in addition to the LAA ostial maximal width, the perimeter measurements had the best correlation results with the closure disk of the LAmbre™ occluder among all the parameters of the LAA orifice; (2) our in-vitro simulation experiments based on 3D printing models showed that comprehensive assessment of the LAA ostial perimeter and maximal width of 3D model based on 3D TEE and CT dataset could help to select the suitable occluder size for one try, especially for the cases when the ratio of the maximal width to the minimal width of the LAA orifice were > 1.4.

Comparison of 3D TEE and CT

At present, the maximal diameter of the LAA orifice is primarily measured by conventional 2D TEE and intraoperative x-ray angiography. However, studies have shown that the measurements of this parameter obtained by multi-planar sampling of 2D TEE were smaller than those obtained by 3D TEE and CT. 3D TEE and cardiac CT are convenient for obtaining full volume data and presenting a full-view image of the LAA via specialized segmentation software. Using these methods, effective measurement was carried out, which was more accurate than 2D-TEE by virtue of the limited sections. And more other parameters of LAA orifice, such as perimeter, area, the angle of the first bend and the distance from the first bend of the LAA to the orifice, can be easily measured and evaluated, which can not be reached by conventional 2D TEE and x-ray angiography. Cardiac CT angiography [13–15] and 3D TEE [16, 17] are both the data source of 3D-printed LAA model, and CT is the mainstream data source. The former has the advantages of clear boundary definitions, superior spatial resolution and the function of reconstructing the LAA digital model by volume rendering imaging. However, because there are some associated risks such as ionizing radiation and contrast agent allergies, images of some patients may not be obtained. Beyond that, CT has a high negative predictive value in the preoperative detection of thrombus in the LAA, however, the positive predictive value is not high, and it is easy to cause false positive because it is difficult for CT to identify blood stasis and thrombus. The latter has no such limitations. The limitation of TEE is the attenuation of ultrasonic signals in the far field, but which had no influence on the evaluation of the LAA orifice. TEE is the foremost imaging method in preoperative screening, the choice of device type and size, intraoperative monitoring and postoperative follow-up. The

feasibility analysis of the acquisition of good LAA 3D-full-volume images by 3D TEE is as follows: (1) in this retrospective study, we selected the patients with clear imaging to ensure smooth following process; (2) because the size of each pixel provided by 3D TEE for each section ranged from 0.40–0.61 by 0.40–0.561 mm in this study (there were minor differences depending on the sampling methods and the volume), and the size of each pixel is 0.625 by 0.625 mm for each CT section, the spatial resolution of 3D TEE is almost the same as it is for CT of this specific region; (3) in this study, the anatomic structures of the LAA were displayed directly and stereoscopically by a segmentation treatment of Mimics software. Therefore, the reconstruction and comparison of the LAA orifice of 3D models based on echo and CT is of great significance to prove the accuracy of 3D TEE. The study may lay a more solid imaging foundation for the complementary advantages of these two imaging methods. Therefore, the reconstruction and comparison of the LAA orifice of 3D models based on echo and CT is of great significance to prove the feasibility and accuracy of 3D TEE.

This study evaluated the concordance between the two methods by comparing five parameters of the LAA orifice. The results showed that the orifice shapes of the LAA in 41 patients were mostly oval, with round, water-drop and triangular shapes found in a few cases, while no foot shape was found, which was considered to be related to the number of samples selected. The kappa value of 0.742 displays good agreement between 3D TEE and CT. Compared with TEE, the LAA orifice shape via CT could be fuller, because the infiltration of contrast media into myocardium may occur in the latter. Despite the slight underestimation of LAA orifice parameter using 3D TEE compared to CCTA, which can possibly be explained by the different working principles of these two techniques, the results still showed a high level of consistency. The comparison results related to simulation operations were showed in the following section.

Comparison of the LAA ostial parameters measurements of 3D models and the final occluder size

The LAA landing zone is defined as the entryway into the dominant lobe of the LAA, where a potential occluder could comfortably and safely be seated within the confines of the body of the LAA. The cases that we studied all used the LAmbre™ device [18, 19], which is a nitinol-based, self-expanding device comprising a hook-embedded umbrella and a cover that is 4–6 mm larger in diameter than the umbrella (Fig. 6). This type of occluder is available in 11 different sizes based on the lobe diameter, which is 16–36 mm, stepwise in 2 mm increments, and the corresponding size of perimeter is 50.3–113.1 mm, stepwise in 6.3 mm increments.

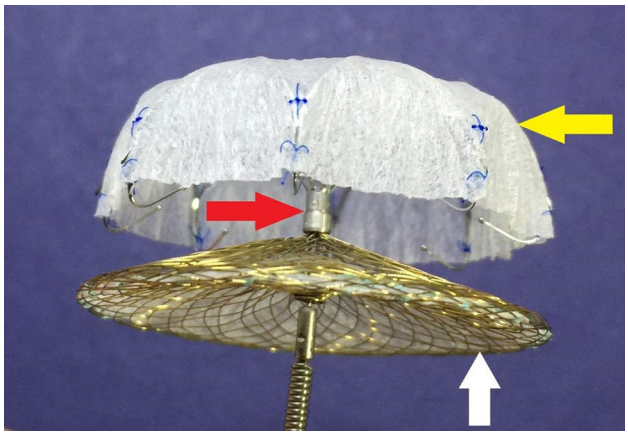

Fig. 6 The LAmbre™ device, which is a nitinol-based, self-expanding device comprising a hook-embedded umbrella (yellow arrow) and a cover (white arrow) connected with a center stick (red arrow)

Similar to ACP occluders [20], the LAmbre™ device has a double-disk structure; therefore, the definition of the landing zone diameters for endoluminal devices is similar to that for the LAmbre™ device. On our digital reconstruction by Mimics based on 3D TEE and CT, the plane of the LAA orifice was reconstructed ~ 10 mm distally from the ostial plane into the lobe [21], and then the maximal width, minimal width, perimeter and area of the LAA landing zone were measured and compared with the size of the closure disk of the LAmbre™ device.

The shapes of the LAA orifice are mostly elliptical or irregular, however, the current occluders are all designed to be round [22, 23]. Self-expansion of the LAmbre™ device may cause deformation of the LAA orifice; for example, the triangular shape becomes oval. After occluder implantation, the morphological deformation of the LAA orifice may lead to marked changes of LAA maximal width and minimal width, but not very noticeable changes of LAA perimeter. The trend and degree of the change in LAA maximal width and minimal width may be determined by the shape of the LAA orifice. Moreover, by virtue of the law that the area of the circle is largest under the condition of constant perimeter, the area of the LAA orifice would increase. Thus, the perimeter may be the most reproducible parameter for sizing devices. Since the minimal width of the LAA orifice is only related to the opening shape, the correlation between it and the device size was not analyzed. Our study shows good correlation to the measurements of the perimeter and maximal width of the LAA orifice by 3D TEE and CT DICOM dataset and the closure disk of the LAmbre™ device, which indicates that these two LAA ostial parameters are both important parameters for the choice of occluder size.

The value of the LAA ostial perimeter of 3D printed models with a rubber-like material in device size selection

Patient-specific 3D LAA models acting as life-like replicas generated by 3D printing could assist the interventional doctor in selecting the proper occluder and thus guide the LAA occlusion [24], and it could help to reconstruct the actual operation to solve intraoperative problems. Moreover, the models may provide the important reference significance to future improvement of occluders and the design of new devices. In this study, we used rubber-like material to make the LAA wall models, its elasticity and softness were similar to human heart tissue, which could well mimics the deformation of the LAA orifice after device implantion. On this basis, we could better explore the relationship between the LAA ostial parameters which would be changed with the LAA orifice shape and the size of the finally selected occluders.

In our in vitro simulation experiments, the LAA occluder sizes of four models based on 3D TEE dataset and two models based on CT dataset were both overestimated just by the analysis of the LAA ostial maximum diameter for the first time. In these six 3D printed models, the orifice shapes were long oval or water drop-like, and the minimal width was relatively small when compared with other ostial shapes. Additionally, in consideration of the above correlation analysis results, other parameters of the orifice should also be analyzed, especially the perimeter. After assistant analysis of the LAA ostial perimeter, this study successfully selected the optimal size of the occluders by simulating the occlusion in the 3D printed LAA models, which were the same as the choices of actual operation. In other two 3D printed LAA models based on CT, the device sizes seleted by both the maximal width and perimeter of the LAA orifice were the same sizes as the actually inserted ones. The reason for the difference between 3D TEE and CT was the way these two imaging methods work as mentioned above. In conclusion, the in vitro release experiment of occluders showed that, when the ratio of the maximal width to the minimal width of the LAA orifice were above 1.4, in other words, when the shape of the LAA orifice is flater, the comprehensive assessment of the maximal width and perimeter of LAA orifice based on both 3D TEE and CT may assist the choice of occluder size to reduce the times of device replacement in practice. Based on the above results, 3D-TEE could be the preferred method in the whole process of the future LAA occlusion to reduce medical cost. For patients with contraindications to TEE or unclear images acquired before surgery, CT can be considered for preoperative evaluation to guide the selection of occluders.

This study found that the results of the orifice parameters of the four 3D printed LAA models were consistent with the results of the 3D reconstruction models in occluder size decision, indicating that the ostial planes defined by these two modes were consistent, and that the printing error of the 3D printed heart wall models was small. In the future work, for the LAA with special ostial shape evaluated by 3D reconstruction model, the measurement and evaluation of the LAA orifice parameters of 3D printed wall models and the simulation operation on them may help to the appropriate device size selection strategy.

Limitations

We report a single-center experience with a small sample size including only 41 individuals. A 3D LAA model was printed within 6 h using a 3D printer, which is time consuming. The depth and angulation of LAA are also important parameters for the choice of the occluder device type. However, we focused on discussing the value of different LAA orifice parameters especially perimeter for sizing an LAA occluder and didn't analysis these parameters in this study. In addition, due to the selection method of device size, the results of good correlation between 3D TEE and actually inserted occluder size were a natural result. This is an inadequacy of the study.

Conclusions

Considering the deformation of the LAA orifice after occluder insertion, for the LAA with special ostial shape, the assessment of the LAA ostial perimeter of 3D model based on 3D TEE and the simulation on 3D printed model with rubber-like material may help to choose the optimal device size of LAmbre™ in increasing the one-time success rate of operation.

Funding This study was supported by a grant from the National Natural Science Fundation of China (Grant No. 81771849).

Compliance with ethical standards

Conflict of interest All authors have no conflict of interest to declare.

Ethical approval All procedures performed in studies involving human participants were in accordance with the ethical standards of the Institutional Review Board of the Einstein Healthcare Network and with the 1964 Helsinki declaration and its later amendments or comparable ethical standards.

Informed consent Informed consent was obtained from all individual participants included in the study.

References

1. Belgaid DR, Khan Z, Zaidi M, Hobbs A (2016) Prospective randomized evaluation of the watchman left atrial appendage closure device in patients with atrial fibrillation versus long-term warfarin therapy: the PREVAIL trial. Int J Cardiol 219:177–179. https://doi.org/10.1016/j.ijcard.2016.06.041
2. MJ Ramos Ramirez, Young B, Harjai K, Mascarenhas V, Vijayaraman P (2017) Left atrial appendage occlusion: in review. J Interv Cardiol 30:448–456. https://doi.org/10.1111/joic.12410
3. Nishimura M, Sab S, Reeves RR, Hsu JC (2018) Percutaneous left atrial appendage occlusion in atrial fibrillation patients with a contraindication to oral anticoagulation: a focused review. Europace 9:1412–1419. https://doi.org/10.1093/europace/eux313
4. Beigel R, Wunderlich NC, Ho SY, Arsanjani R, Siegel RJ (2014) The left atrial appendage: anatomy, function, and noninvasive evaluation. JACC Cardiovasc Imaging 7:1251–1265. https://doi.org/10.1016/j.jcmg.2014.08.009
5. Otton JM, Spina R, Sulas R, Subbiah RN, Jacobs N, Muller DW, Gunalingam B (2015) Left atrial appendage closure guided by personalized 3d-printed cardiac reconstruction. JACC Cardiovasc Interv 8:1004–1006. https://doi.org/10.1016/j.jcin.2015.03.015
6. Goitein O, Fink N, Guetta V, Beinart R, Brodov Y, Konen E, Goitein D, Di Segni E, Grupper A, Glikson M (2017) Printed MDCT 3D models for prediction of left atrial appendage (LAA) occluder device size: a feasibility study. EuroIntervention. 13(9):e1076–e1079. https://doi.org/10.4244/EIJ-D-16-00921
7. Goitein O, Fink N, Hay I, Di Segni E, Guetta V, Goitein D, Brodov Y, Konen E, Glikson M (2017) Cardiac CT Angiography (CCTA) predicts left atrial appendage occluder device size and procedure outcome. Int J Cardiovasc Imaging 33:739–747. https://doi.org/10.1007/s10554-016-1050-6
8. Vukicevic M, Mosadegh B, Min JK, Little SH (2017) Cardiac 3D Printing and its Future Directions. JACC Cardiovasc Imaging 10:171–184. https://doi.org/10.1016/j.jcmg.2016.12.001
9. Olejník P, Nosal M, Havran T, Furdova A, Cizmar M, Slabej M, Thurzo A, Vitovic P, Klvac M, Acel T, Masura J (2017) Utilisation of three-dimensional printed heart models for operative planning of complex congenital heart defects. Kardiol Pol 75:495–501. https://doi.org/10.5603/KP.a2017.0033
10. Hadeed K, Acar P, Dulac Y, Cuttone F, Alacoque X, Karsenty C (2018) Cardiac 3D printing for better understanding of congenital heart disease. Arch Cardiovasc Dis 111(1):1–4. https://doi.org/10.1016/j.acvd.2017.10.001
11. Iriart X, Ciobotaru V, Martin C, Cochet H, Jalal Z, Thambo JB, Quessard A (2018) Role of cardiac imaging and three-dimensional printing in percutaneous appendage closure. Arch Cardiovasc Dis 111(6–7):411–420. https://doi.org/10.1016/j.acvd.2018.04.005
12. Ciobotaru V, Combes N, Martin CA, Marijon E, Maupas E, Bortone A, Bruguière E, Thambo JB, Teiger E, Pujadas-Berthault P, Ternacle J, Iriart X (2018) Left atrial appendage occlusion simulation based on three-dimensional printing: new insights into outcome and technique. EuroIntervention 14(2):176–184. https://doi.org/10.4244/EIJ-D-17-00970
13. Obasare E, Mainigi SK, Morris DL, Slipczuk L, Goykhman I, Friend E, Ziccardi MR, Pressman GS (2018) CT based 3D printing is superior to transesophageal echocardiography for preprocedure planning in left atrial appendage device closure. Int J Cardiovasc Imaging 34(5):821–831. https://doi.org/10.1007/s10554-017-1289-6
14. Hell MM, Achenbach S, Yoo IS, Franke J, Blachutzik F, Roether J, Graf V, Raaz-Schrauder D, Marwan M, Schlundt C (2017) D printing for sizing left atrial appendage closure device: head-to-head comparison with computed tomography and transesophageal echocardiography. EuroIntervention. https://doi.org/10.4244/EIJ-D-17.
15. Wang DD, Eng M, Kupsky D, Myers E, Forbes M, Rahman M, Zaidan M, Parikh S, Wyman J, Pantelic M, Song T, Nadig J, Karabon P, Greenbaum A, O'Neill W (2016) Application of 3-dimensional computed tomographic image guidance to WATCHMAN implantation and impact on early operator learning curve: single-center experience. JACC Cardiovasc Interv 9:4129–4140. https://doi.org/10.1016/j.jcin.2016.07.038
16. Liu P, Liu R, Zhang Y, Liu Y, Tang X, Cheng Y (2016) The value of 3D printing models of left atrial appendage using real-Time 3D transesophageal echocardiographic data in left atrial appendage occlusion: applications toward an era of truly personalized medicine. Cardiology 135(4):255–261. https://doi.org/10.1159/000447444
17. Li H, Qingyao Bingshen, Shu M, Lizhong Wang X, Song Z (2017) Application of 3D printing technology to left atrial appendage occlusion. Int J Cardiol 15(411):258–263. https://doi.org/10.1016/j.ijcard.2017.01.031
18. Saw J, Percutaneous Lempereur M (2014) Left atrial appendage closure: procedural techniques and outcomes. JACC Cardiovasc Interv 7:1205–1220. https://doi.org/10.1016/j.jcin.2014.05.026
19. Cruz-González I, Freixa X, Fernández-Díaz JA, Moreno-Samos JC, Martín-Yuste V, Goicolea J (2018) Left Atrial Appendage Occlusion With the LAmbre Device: Initial Experience. Rev Esp Cardiol (Engl Ed) 71(9):755–756. https://doi.org/10.1016/j.rec.2017.04.015
20. De Backer O, Arnous S, Ihlemann N, Vejlstrup N, Jørgensen E, Pehrson S, Krieger TD, Meier P, Søndergaard L, Franzen OW (2014) Percutaneous left atrial appendage occlusion for stroke prevention in atrial fibrillation: an update. Open Heart 1:e000020. https://doi.org/10.1136/openhrt-2013-000020
21. Wunderlich NC, Beigel R, Swaans MJ, Ho SY, Siegel RJ (2015) Percutaneous interventions for left atrial appendage exclusion: options, assessment, and imaging using 2D and 3D echocardiography. JACC Cardiovasc Imaging 8:472–488. https://doi.org/10.1016/j.jcmg.2015.02.002
22. Piccini JP, Sievert H, Patel MR (2017) Left atrial appendage occlusion: rationale, evidence, devices, and patient selection. Eur Heart J 38(12):869–876. https://doi.org/10.1093/eurheartj/ehw330
23. Yu CM, Khattab AA, Bertog SC, Lee AP, Kwong JS, Sievert H, Meier B (2013) Mechanical antithrombotic intervention by LAA occlusion in atrial fibrillation. Nat Rev Cardiol 10:707–722. https://doi.org/10.1038/nrcardio.2013.158
24. Goitein O, Fink N, Guetta V, Beinart R, Brodov Y, Konen E, Goitein D, Di Segni E, Grupper A, Glikson M (2017) Printed MDCT 3D models for prediction of left atrial appendage (LAA) occluder device size: a feasibility study. EuroIntervention 13:e1076–e1079. https://doi.org/10.4244/EIJ-D-16-00921